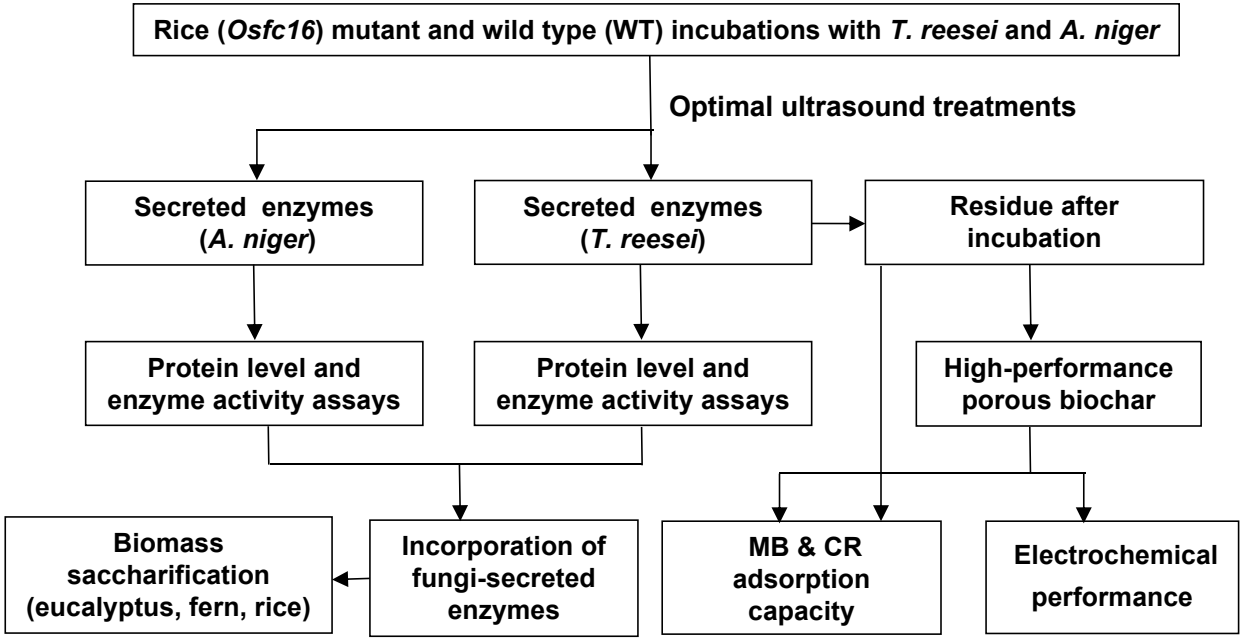

Fig. S1. General experimental procedure of fungal incubation with rice straw under optimal ultrasound treatments for secreting cellulases and sugars and generating biochar for dye adsorption and electrochemical performance.

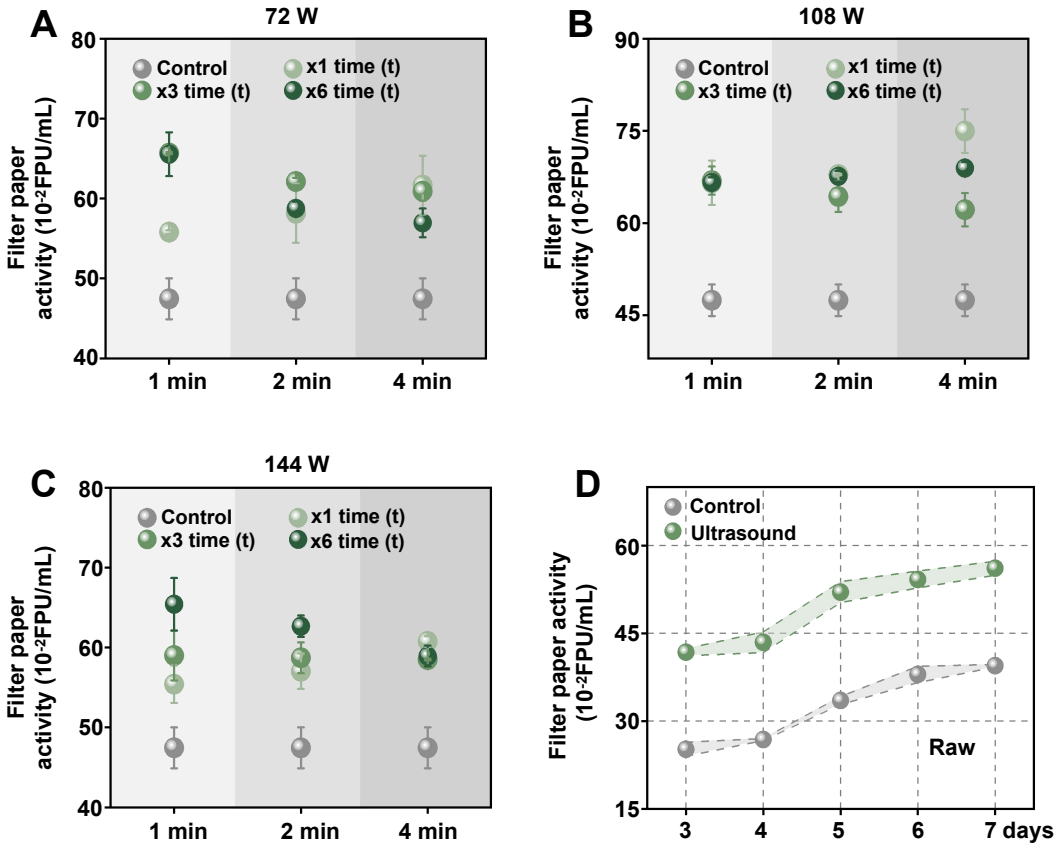

Fig. S2. *T. reesei* incubation with rice (wild type) straw for enzymes secretion under various ultrasound treatments: (a-c) Filter paper activities/FPAs of secreted solutions under ultrasound treatments at 72/108/144 W power for 1, 2, 4 min under 1, 3 and 6 times repeating; (d) FPAs of secreted solutions under ultrasound treatments at 108 W frequency for 4 min under 1 time repeating with WT rice straw on 3-7 days.

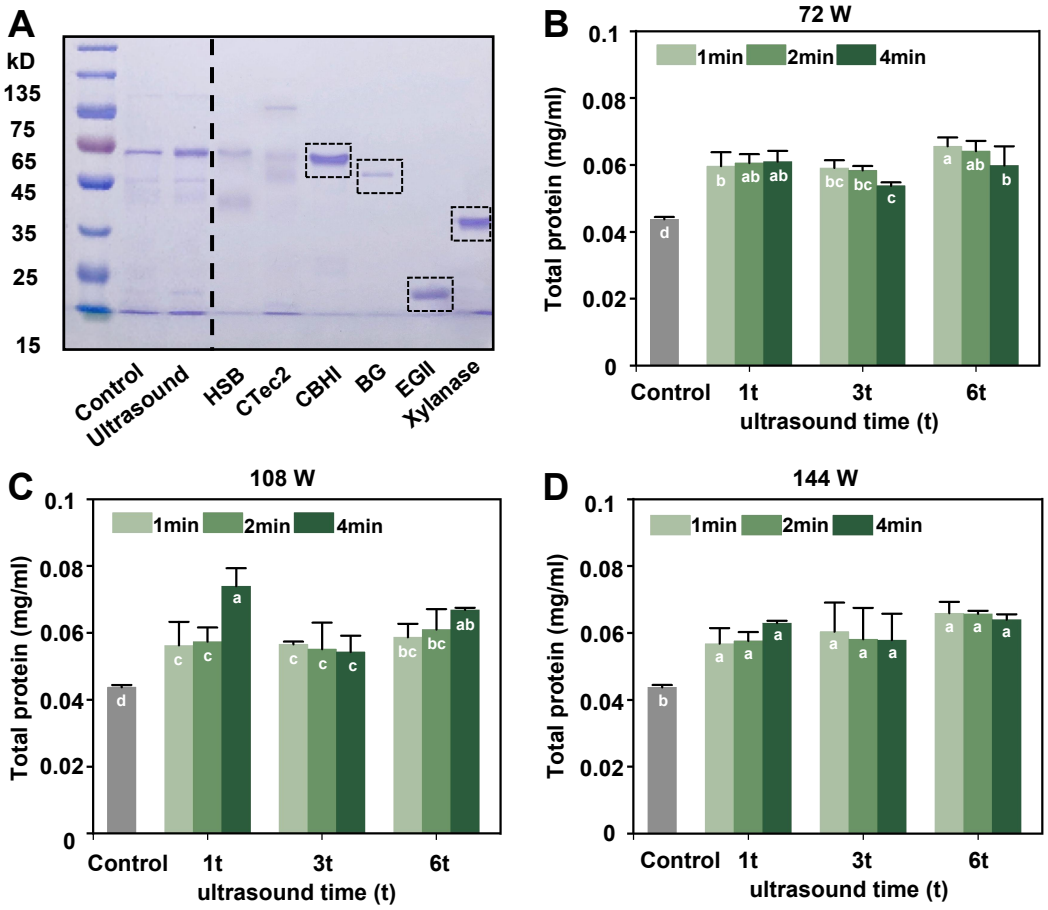

Fig. S3. Characterization of enzymes solutions secreted from *T. reesei* incubation with rice (wild type) straw under ultrasound treatments: (a) SDS-PAGE protein profiling of secreted solutions, boxes highlighted for standard individual enzymes (CBHI, BG, EGII, xylanases), HSB and CTec2 as two commercial companies for mixed-cellulases; (b-d) Total protein content of secreted solutions. Significant differences between samples were determined using one-way ANOVA: $p < 0.05$ (n=10).

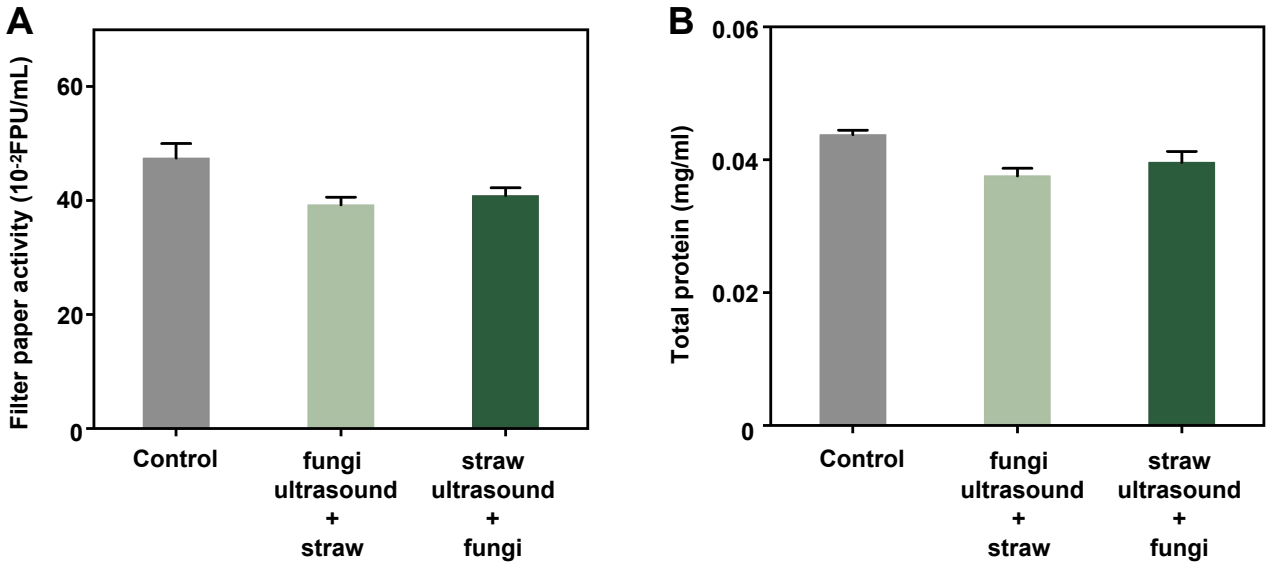

Fig. S4. Characterization of FPAs activity and total protein levels of *T. reesei*–secreted solutions after incubation for 7 days: “fungi ultrasound + straw” as only one time of optimal ultrasound treatment with *T. reesei* before incubation with rice (WT) straw substrate, “straw ultrasound + fungi” as only one time of optimal ultrasound treatment with WT straw substrate before incubated with *T. reesei* strain.

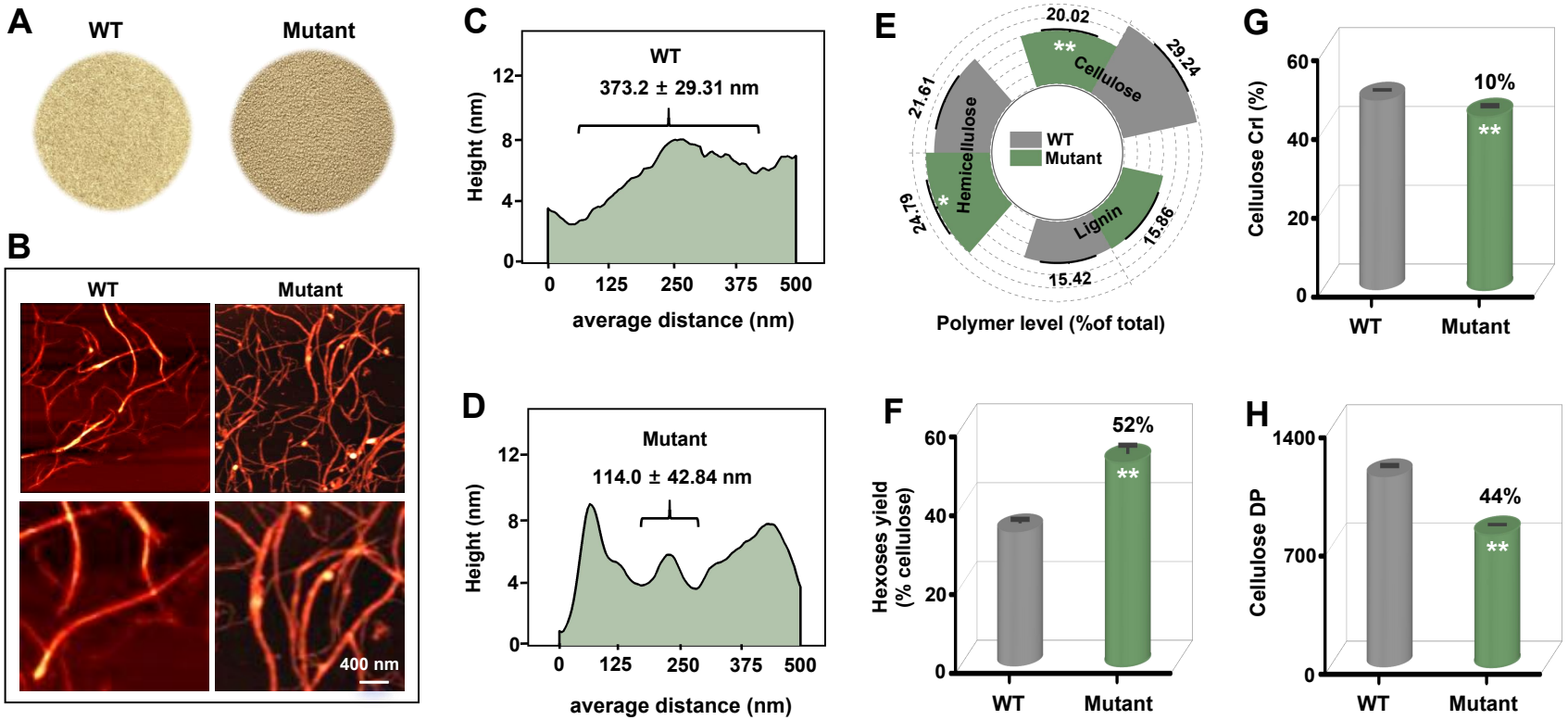

Fig. S5. Characterization of rice mutant (*Osfc16)* and wild type (WT): (a) Mature rice straw powder; (b) AFM images of cellulose nanofibrils (CNFs) assembly; (c, d) Evaluation of average distance between two defects on the surfaces of CNFs as highlight (b) to present nanofibrils length on average (n=50); (e) Wall polymer levels; (f) Hexoses yield released from enzymatic hydrolysis; (g) Cellulose crystalline index (CrI); (h) Degree of polymerization (DP); * and ** As significant difference between mutant and WT at $p < 0.05$ and 0.01 levels (n=3), bar as means ± SD.

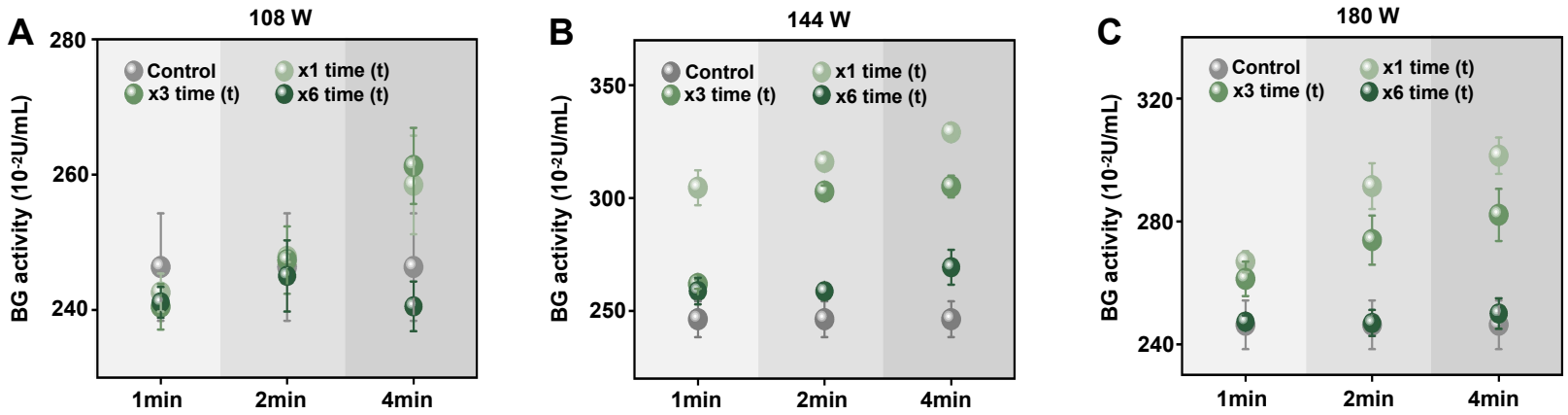

Fig. S6. BG activity of secreted solutions from *A. niger* incubation with rice (WT) straw under various ultrasound treatments at 108/144/180 W power for 1 min, 2 min and 4 min under 1, 3 and 6 times repeating.

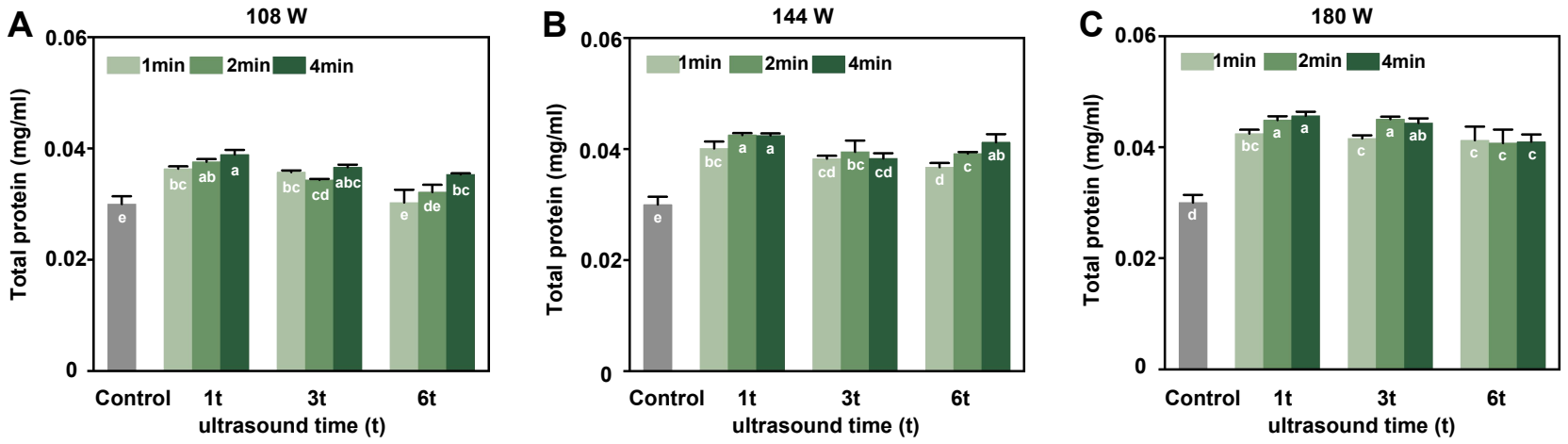

Fig. S7. Total protein content of secreted-solution from *A. niger* incubation with rice (wild type) straw under various ultrasound at 108/144/180 W power for 1 min, 2 min and 4 min under 1, 3 and 6 times repeating. Significant differences between samples were determined using one-way ANOVA: $p < 0.05$ (n=10).

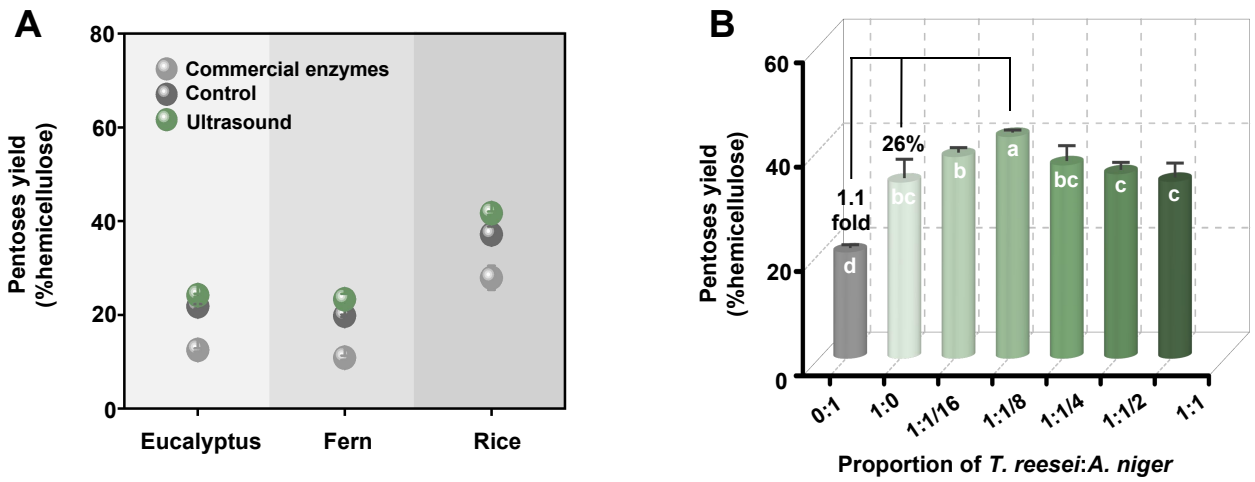

Fig. S8. Characterization of biomass saccharification in three bioenergy crops: (a) Pentoses yield released from enzymatic hydrolysis under 0.5% NaOH pretreatment using *T. reesei*-secreted enzymes and commercial enzymes; (b) Pentoses yield released from enzymatic hydrolyses by incorporating *T. reesei*-secreted enzymes and *A. niger*-secreted enzymes at different proportions. Control as secreted enzymes from fungal incubation without ultrasound treatment; Significant differences between samples were determined using one-way ANOVA: $p < 0.05$ (n=7).

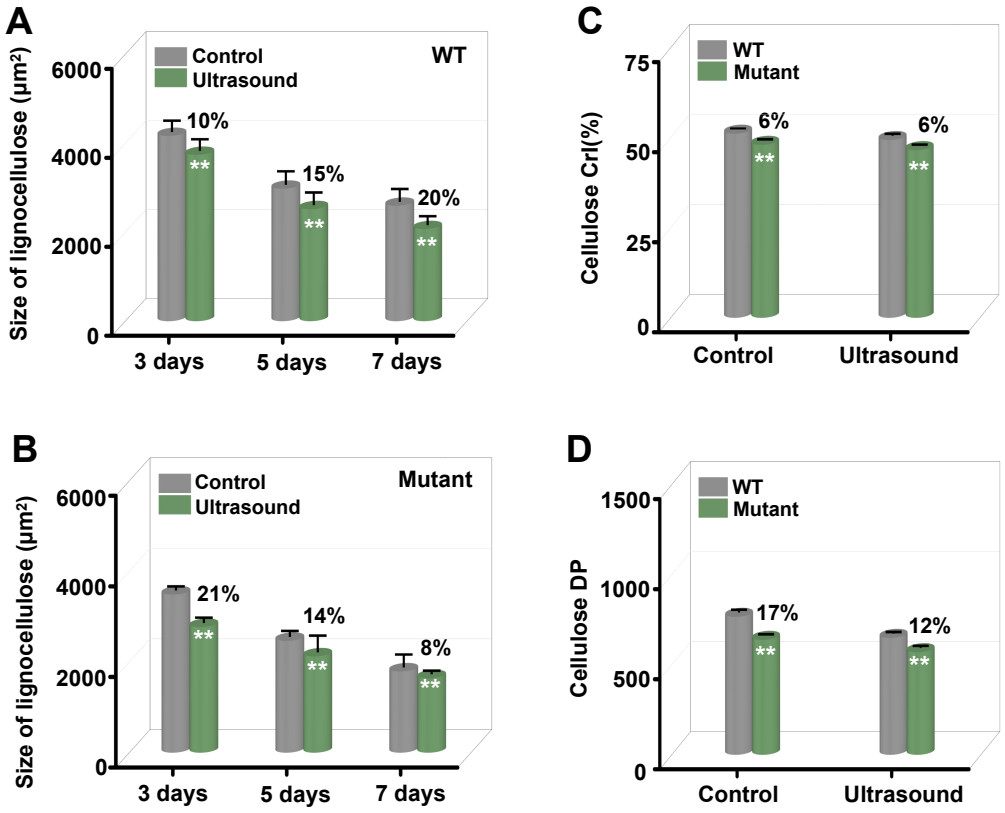

Fig. S9. Characterization of lignocelluloses from *A. niger* incubation with rice mutant and WT straw under optimal ultrasound treatment relative to the control (without ultrasound): (a, b) Size of randomly-selected 30 lignocellulose substrates on average (n=30); (c, d) CrI and DP values of lignocellulose substrates (n=3). ** As significant difference between mutant and WT or ultrasound treatment and control at $p < 0.01$ level, bar as means ± SD.

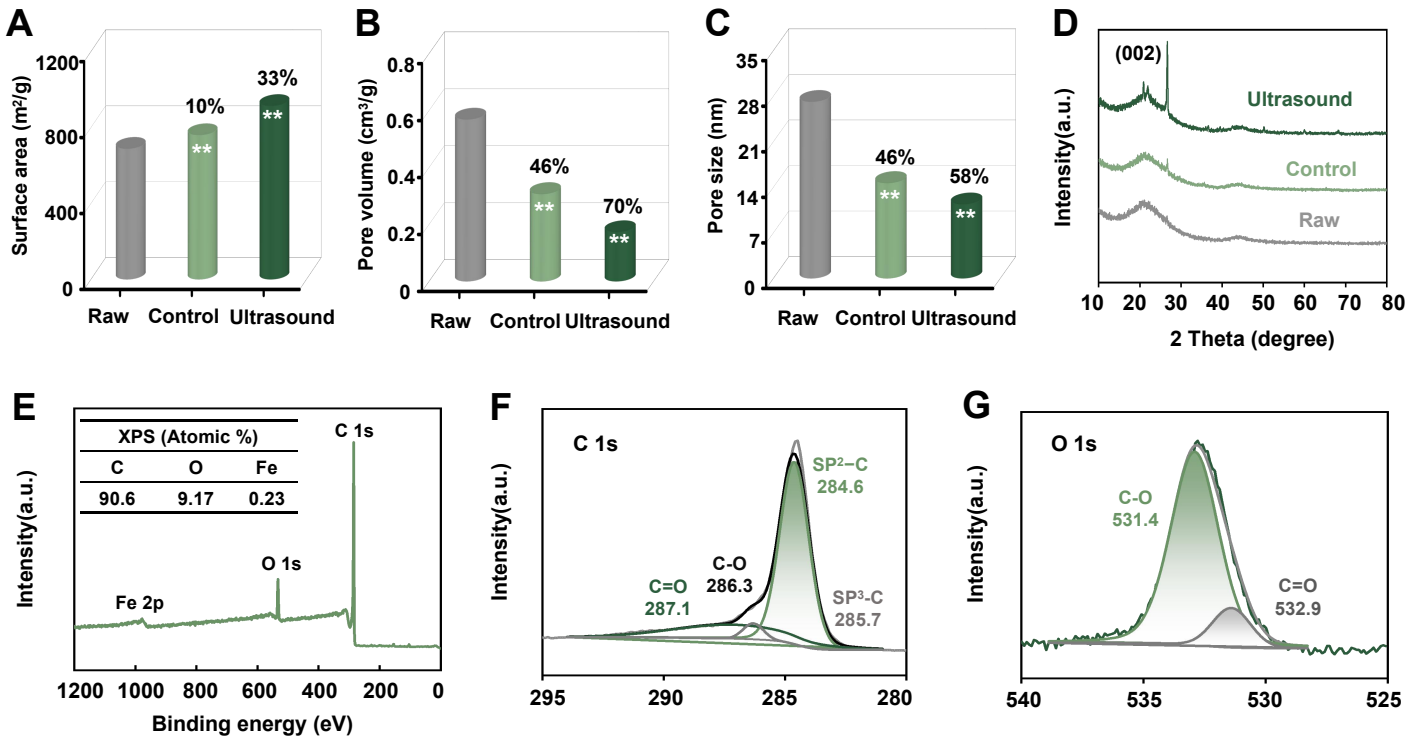

Fig. S10. Characterization of the biocarbon generated from lignocellulose residues after *T. reesei* incubation with rice mutant straw under optimal ultrasound treatment relative to the control (without ultrasound): (a-c) Surface area, pore volume and size from BET assay; (d) XRD assay; (e) XPS spectra profiling; (f, g) High-resolution XPS spectrum at C1s and O1s region; Raw as biocarbon sample directly generated from rice raw straw; **As significant difference relative to Raw sample at $p < 0.01$ level (n=3), bar as means ± SD.

Table S1 LC-MS/MS assay of *T. reesei*-secreted enzymes incubated with rice mutant under optimal ultrasound treatment.

Protein Name	Accession No.	Coverage [%]	Peptides	Razor+ unique peptides	Unique peptides	Intensity A	MW[kDa]
Cellobiohydrolase I	A0A024RXP8	12.26	5	5	5	1721520	54.11
Cellobiohydrolase II	A0A024SH76	16.56	7	7	7	597238	49.65
Endo-β-1,4-glucanase I	A0A024SNB7	2.83	1	1	1	303764	48.21
Endo-β-1,4-Glucanase VII	A0A024SFJ2	10.44	3	3	3	685189	26.80
β-glucosidase I	A0A024SB94	9.22	7	6	6	5694.18	84.68
β-glucosidase II	A0A024SD46	15.2	11	11	11	6915.28	93.65
Endo-1,4-β-xylanase III	A0A024SIB3	16.43	6	6	6	1143830	38.08
Xyloglucanase	A0A024S9Z6	14.92	10	10	10	358007	87.13
Swollenin	A0A024RZP7	8.32	3	3	3	129227	51.52

Table S2 Volumetric activity (U/mL) and specific activity (U/mg protein) of lignocellulose-degradation enzymes from *T. reesei* incubation with rice (mutant) straw under optimal ultrasound treatments and commercial commercial enzymes HSB.

Samples	Volumetric activity (U/mL)				Specific activity (U/mg protein)			
	CBHI	EGII	BG	Xylanase	CBHI	EGII	BG	Xylanase
Commercial enzymes (HSB)	0.02	5.37	-	121	0.55	162.73	-	3666.67
Control	0.08	6.06	0.01	285.8	2.27	183.73	0.39	8660.61
Ultrasound	0.13	6.63	0.02	311.1	3.97	200.76	0.7	9427.27

Table S3 Estimation of global hexoses and pentoses yields (/ha/year) in two bioenergy crops using secreted-enzymes from *T. reesei* incubation with rice mutant straw under optimal ultrasound treatment relative to the control (without ultrasound) based on laboratory-scale data.

Samples	Biomass yield (/ha/year)	Hexoses yield (/ha/year)		Pentoses yield (/ha/year)		References
		Control	With ultrasound treatments	Control	With ultrasound treatments	
Eucalyptus	21.6 t (ton) (every 36 m^3)	1.28 t	1.95 t	1.03 t	1.14 t	Elli et al., 2019
Rice	4530 t (worldwide)	1031.53 t	1187.15 t	387.07 t	434.37 t	Xu et al., 2022

These values are illustrative scenarios. Actual achievable yields at scale would be subject to numerous technical, economic, and logistical factors not considered here and require full techno-economic (TEA) and life-cycle (LCA) assessment.

Table S4 Characteristic chemical bonds of the FT-IR spectra presented in Fig. 5F.

Reported wave number (cm^{-1})	Observed wave number (cm^{-1})	Functional group	Assignment	References
898	897	C—H vibration	Cellulose	Ong et al., 2020
1045	1045	C-O-C	Cellulose	Cai et al., 2019
1163	1164	C-O-C asymmetric stretching	Cellulose	Guo et al., 2016
1247	1245	C—O—C stretching of aryl-alkyl ether	Lignin	Ong et al., 2020
1373	1368	C-H_2 scissoring	Cellulose	Balat et al., 2011
1515	1510	C=C stretching of the aromatic ring	Lignin	Xu et al., 2014
1632	1636	-C=O stretching from CO-OR	Pectin	Baum et al., 2016